Biochem1991

DATASET · FEBRUARY 2013

READS
22

10 AUTHORS, INCLUDING:

Palayakotai Raghavan
Nanorx Inc
26 PUBLICATIONS **58** CITATIONS
SEE PROFILE

Peter Farina
Canaan Partners
28 PUBLICATIONS **598** CITATIONS
SEE PROFILE

A Novel Dipyridodiazepinone Inhibitor of HIV-1 Reverse Transcriptase Acts through a Nonsubstrate Binding Site

Joe C. Wu,*,‡ Thomas C. Warren,‡ Julian Adams,§ John Proudfoot,§ Jerry Skiles,§ Palayakotai Raghavan,§ Clark Perry,§ Ian Potocki,§ Peter R. Farina,‡ and Peter M. Grob‡

Departments of Biochemistry and Medicinal Chemistry, Boehringer Ingelheim Pharmaceuticals, Inc., 90 East Ridge, P.O. Box 368, Ridgefield, Connecticut 06877

Received September 17, 1990; Revised Manuscript Received December 5, 1990

ABSTRACT: A novel dipyridodiazepinone, 6,11-dihydro-11-cyclopropyl-4-methyldipyrido[2,3-*b*:2′,3′-*e*]-[1,4]diazepin-6-one (BI-RG-587), is a selective noncompetitive inhibitor of HIV-1 reverse transcriptase (RT-1). An azido photoaffinity analogue of BI-RG-587 was synthesized and found to irreversibly inhibit the enzyme upon UV irradiation. BI-RG-587 and close structural analogues competitively protected RT-1 from inactivation by the photoaffinity label. A thiobenzimidazolone (TIBO) derivative, a nonnucleoside inhibitor of RT-1, also protected the enzyme from photoinactivation, which suggests a common binding site for these compounds. Substrates dGTP, template-primer, and tRNA afforded no protection from enzyme inactivation. A tritiated photoaffinity probe was found to stoichiometrically and selectively label p66 such that 1 mol of probe inactivates 1 mol of RT-1.

The transcription of viral RNA to proviral DNA by the enzyme reverse transcriptase (RT-1)[1] is a requisite step in the life cycle of human immunodeficiency virus 1 (HIV-1) (Fauci, 1988). Progress has been made in the development of chemotherapeutic agents such as the nucleoside analogue 3′-azido-2′,3′-dideoxythymidine (AZT), which acts on the enzyme, after cellular phosphorylation, as a chain terminator (De Clercq, 1990). Unfortunately, cellular toxicity and viral resistance limit its effectiveness (Richman et al., 1987; Larder & Kemp, 1989). Other nucleoside analogues such as 2′,3′-dideoxyinosine (ddI) and 2′,3′-dideoxycytidine (ddC) are in clinical trials and may offer some advantages over AZT (Hoa et al., 1988; DeClercq, 1989). Recently, a novel, potent nonnucleoside inhibitor of RT-1 was described (Merluzzi et al., 1990). This compound, BI-RG-587 (**1**), is a dipyridodiazepinone that inhibits RT-1 in a noncompetitive manner with respect to dGTP (K_i = 200 nM) (see Chart I). HIV-1 antiviral activity has been demonstrated in vitro (IC_{50} = 40 nM) as measured by p24 production, in situ hybridization, and the lack of syncytia formation in cultured human T cell lines and freshly isolated human peripheral blood lymphocytes. BI-RG-587 displays a high degree of specificity for RT-1 in comparison to other human DNA polymerases, α, β, γ, and δ, as well as feline and simian reverse transcriptases. This specificity is further evident from the observation that HIV-2 replication is not inhibited by the presence of **1**. Interestingly, Pauwels et al. (1990) have described a series of thiobenzimidazolones (TIBO derivatives) that are also nonnucleoside inhibitors of RT-1 and share some of the properties associated with compound **1**, particularly the lack of activity against HIV-2 (Merluzzi et al., 1990).

In order to investigate the interaction of **1** with RT-1, we have synthesized a structurally related photoaffinity label (**2**) and a tritiated analogue (**3**). These compounds have been specifically employed to understand the inhibitory mechanism by determining the stoichiometry for inhibition and by localizing the binding to the RT-1 heterodimer (p66/p51). In addition, we have used the photoaffinity probes to establish that dipyridodiazepinones and a TIBO compound (**4**) share a common binding site [RT-1 modulatory site (RT_1MS)].

Chart I

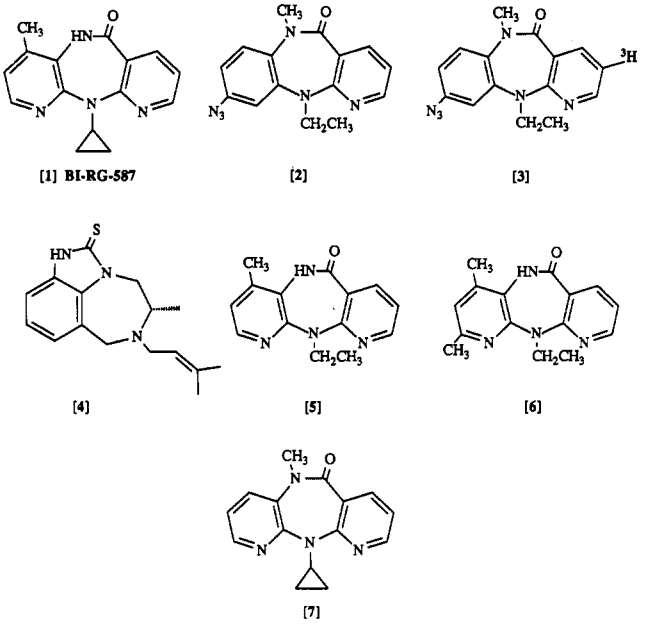

Materials and Methods

Synthetic template poly(rC) (about 2000 bases), primer oligo(dG) (12–18 mer), Q-Sepharose fast-flow, and a Beta Plate scintillation counter were obtained from LKB Pharmacia (Piscataway, NJ). Nonradioactive deoxynucleoside triphosphates, yeast tRNA, trichloroacetic acid, dithiothreitol (DTT), sodium pyrophosphate, Tris, bovine serum albumin

* To whom correspondence should be addressed.
‡ Department of Biochemistry.
§ Department of Medicinal Chemistry.

[1] Abbreviations: RT, reverse transcriptase; TIBO, thiobenzimidazolone; HIV-1, human immunodeficiency virus 1; AZT, 3′-azido-2′,3′-dideoxythymidine; ddI, 2′,3′-dideoxyinosine; ddC, 2′,3′-dideoxycytidine; DTT, dithiothreitol; PCR, polymerase chain reaction; PBL, peripheral blood leukocytes; BSA, bovine serum albumin.

0006-2960/91/0430-2022$02.50/0

(BSA), and Kodak XRA-5 X-ray film were purchased from Sigma (St. Louis, MO). Tritiated dGTP (12 Ci/mmol) was from Du Pont/NEN Research Products, and Amplify was obtained from Amersham (Arlington, IL). *Escherichia coli* (strain JM 109) transformed with pKRT 2 was obtained from Dr. W. Summers, Yale University (D'Aquila & Summers, 1989), and is also available from the NIH Aids Research and Reference Reagent Program Catalog (catalog no. 393). λ HIV-2_{rod} was obtained from the NIH Aids Research and Reference Reagent Program Catalog (catalog no. 207). P-11 phosphocellulose exchanger was purchased from Whatman (Hillsboro, OR). BCA reagent was from Pierce (Rockford, IL), and no. 30 glass fiber filters were from Schleicher & Schuell (Keene, NH). The TSK phenyl 5-PW 150 × 15 mm HPLC column was from Phenomenex (Torrence, CA), and YM-30 membranes were obtained from Amicon (Danvers, MA). The Hi-Pore RP-304 250 × 4.6 mm HPLC column, acrylamide, bis(acrylamide), sodium dodecyl sulfate, TEMED, Coomassie Blue R-250, and glycine were purchased from Bio-Rad (Richmond, CA). All other chemicals were of reagent grade.

Synthesis of Photoaffinity Labels. A more detailed description of the preparation of BI-RG-587 analogues is presented elsewhere (Hargrave et al., 1991). 9-Azido-5,6-dihydro-11-ethyl-6-methyl-11*H*-pyrido[2,3-*b*][1,5]benzodiazepin-5-one (**2**) was prepared as follows. An equimolar mixture of 2-chloronicotinic acid and 4-nitrophenylenediamine was heated in sulfolane at 170 °C for 5 h. After cooling, the precipitate was collected and washed with hot ethanol. The condensation product, a mixture of 8- and 9-nitro-5,6-dihydro-11*H*-pyrido[2,3-*b*]benzodiazepin-5-ones, was then methylated with methyl iodide and dimsylsodium in DMSO, and the 5,6-dihydro-6-methyl-9-nitro isomer was purified by fractional crystallization. Ethylation with ethyl iodide and dimsylsodium in DMSO followed by stannous chloride reduction of the nitro group gave the 8-amino compound. This was converted to the azide by diazotization with sodium nitrite followed by reaction with sodium azide. The 9-azido derivative **2** was crystallized from diethyl ether to give analytically pure material: mp 115–118 °C; CIMS molecular ion H^+ 295; C, H, and N analysis and spectroscopic characterization were consistent with the structure. A methanolic solution of **2** had a λ_{max} of 248 nm (ϵ = 30 000).

The synthesis of the azido photoaffinity probe **3** labeled at the 3-position with tritium was carried out by a similar procedure, except that 2-chloronicotinic acid was replaced by 2-chloro-5-bromonicotinic acid. The resultant 3-bromoamine intermediate was then allowed to react with 1 Ci of tritium gas in the presence of 10% Pd–C in ethyl acetate. Subsequent diazotization and reaction with potassium azide gave **3**. The HPLC-purified final product was >98% pure (2.02 Ci/mmol) and was stored at −20 °C in the dark.

Preparation of rHIV-1 RT. Recombinant RT-1 was purified from lysates of *E. coli* strain JM 109 containing pKRT 2 encoding for a 66-kDa RT-1 gene product, utilizing a methodology reported in the literature (Mizrahi et al., 1989) with the following modifications. Briefly, lysates were incubated in the absence of protease inhibitors overnight to allow bacterial protease processing of the 66-kDa gene product to the mature p66/p51 heterodimer form to occur. After the inclusion of 2 mM EDTA, lysates were applied to a phosphocellulose column and eluted with a linear 0.1–0.75 M NaCl gradient in 50 mM Tris, pH 8.0. Fractions exhibiting RT activity were pooled, dialyzed, and applied to a Q-Sepharose column and eluted with a linear 0.01–0.35 M NaCl gradient. Active fractions were pooled, concentrated, and diluted with an equal volume of 2 M $(NH_4)_2SO_4$ and chromatographed on a semipreparative TSK phenyl-5PW (HPLC) column with a descending linear 1.0–0.0 M $(NH_4)_2SO_4$ gradient in 0.1 M sodium phosphate, pH 7.0. Fractions were chilled and diluted with equal volumes of 2X storage buffer (100 mM MES, 600 mM KH_2PO_4, 350 mM KCl, 20% glycerol, 0.04% NaN_3, pH 6.0) immediately following elution from the columns. Fractions exhibiting RT activity and devoid of significant contaminating proteins were pooled and concentrated to approximately 1 mg/mL and stored at −80 °C. SDS–PAGE analysis of this enzyme preparation showed 66- and 51-kDa bands in equimolar proportion (1.02:1.0) and greater than 95% purity as determined by reversed-phase HPLC. N-Terminal sequencing confirmed the identity as RT-1, and the specific activity of the final RT-1 preparation was 20–35 nmol of dGMP mg^{-1} min^{-1}.

Preparation of rHIV-2 RT. HIV-2 RT (RT-2) was purified by an identical procedure from lysates of *E. coli* transformed with pKRT 2 plasmid, which contains the p68 RT-2 coding sequence. This construct was subcloned from λ HIV-2_{rod} via PCR and codes for the RT-2 open reading sequence (Guyader et al., 1987). Nucleic acid sequencing of this plasmid, pASRT 2, detected four amino acid substitutions that have been previously reported in HIV-2 isolates. One additional substitution was detected in the RNase H domain; serine 505 is a valine. SDS–PAGE analysis of RT-2 derived by this methodology shows that both subunits exhibit a slightly larger apparent molecular weight compared to RT-1. The low molecular weight subunit of HIV-2 RT (p54) displays minor size heterogeneity, possibly due to variable C-terminal processing. N-Terminal sequencing confirmed the identity of RT-2, and the specific activity of the final RT-2 was approximately equivalent to the RT-1 preparation.

Enzyme Assay. RT-1 and RT-2 activities were routinely assayed by using synthetic template-primers as described (Starnes & Cheng, 1987) with slight modification. Briefly, a 60-μL reaction mixture contained 50 mM Tris-HCl, pH 7.8, 2 mM $MgCl_2$, 1 mM DTT, 0.5 mg/mL BSA, 100 mM NaCl, 1.0 μg/mL poly(rC)$_{2000}$·oligo(dG)$_{12-18}$ with a molar ratio of 1:5, 2.0 μM [^{3}H]dGTP, and 0.5 nM enzyme. After a 60-min incubation at 25 °C, reactions were terminated by the addition of 50 μL of 10% trichloroacetic acid solution containing 2% sodium pyrophosphate. Acid-insoluble material was collected by a Skatron Harvestor (Skatron, Inc., Sterling, VA) on a no. 30 glass fiber filter, and radioactivity was determined by LKB Beta Plate scintillation spectroscopy.

Photoaffinity Labeling of RT-1. Polypropylene microcontainers containing the reaction mixtures were illuminated with a lamp (GE 275-W sun lamp) that provided UV-irradiation intensity of about 15 μW/cm^2. The intensity of the UV light was kept low so that the labeling was gradual enough to be conveniently monitored. Under this illumination setting, k' was found to be 0.071 min^{-1}. During this weak UV illumination, the irreversible inactivation of RT-1 by photoaffinity label **2** or **3** was followed conveniently by removing 1-μL aliquots of the reaction mixture at different times, diluting the sample 1500-fold to dissociate the noncovalently bound probe, and assaying the polymerase activity of each sample. Experimental values of the photoinactivation rate at various concentrations of **2** and its analogues were determined from a pseudo-first-order plot.

SDS–PAGE and Autoradiography. Samples for SDS–PAGE analysis were suspended in Laemmli sample buffer, heated at 95 °C for 3 min, and subjected to 10.0% SDS–

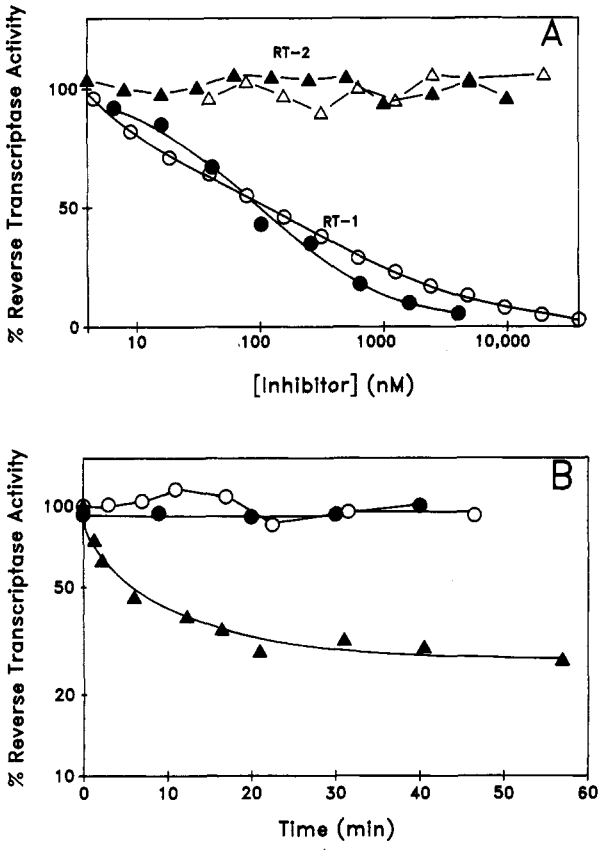

FIGURE 1: Reversible and irreversible inhibition of HIV RT by compounds **1** and **2**. (A) Reversible inhibition in the dark. RT polymerase activity was assayed in a solution containing 0.5 nM RT [(○, ●) RT-1; (△, ▲) RT-2] and 4.5–37 000 nM **1** (●, ▲) or **2** (○, △) (see RT assay method). (B) Irreversible photoinactivation. Solutions containing (▲) 0.4 μM RT-1, 0.5 μM **2**, and 0.5 mg/mL BSA or (○) 0.4 μM RT-1 and 0.5 mg/mL BSA were irradiated with low-intensity UV. The progress of the photoinactivation was monitored by assaying RT-1 activity at indicated illumination times after a 1500-fold dilution. RT-1 incubated with **2** in the dark did not significantly change its activity (●).

polyacrylamide gel electrophoresis (Laemmli, 1970). The gels either were stained with Coomassie Blue R-250, destained, and dried or were fixed in destain (10% acetic acid, 5% methanol, 85% water) for 15 min, treated with Amplify enhancing fluid for 30 min, dried, and exposed to Kodak XRA-5 X-ray film for 4 days at −80 °C. The film was developed with an X-Omat developer (AFP Imaging, Elmsford, NY).

RESULTS

Reversible Inhibition of RT-1 by the Photoaffinity Probe in the Dark. Purified, recombinant HIV-1 RT (RT-1) and HIV-2 RT (RT-2) were treated in the dark with various concentrations of **1** and its photoaffinity analogue **2**. As shown in Figure 1A, RT-1 polymerase activity was inhibited in a dose-dependent fashion by both inhibitors, whereas RT-2 was inhibited by neither. The RT-1 IC_{50} value derived from these data for **1** is 90 nM and for **2** is 160 nM.

Irreversible Inhibition of RT-1 by Photoaffinity Labeling. RT-1 was mixed with the photoaffinity label **2** and irradiated with UV light between 0 and 50 min. The ratio of **2** to enzyme was approximately unity (0.5 vs 0.4 μM), and BSA was present at 0.5 mg/mL. The samples were assayed after a 1500-fold dilution, which dissociated noncovalently bound **2** from the enzyme. Figure 1B shows the results of a typical photolabeling experiment. Enzyme activity remains unchanged with time if enzyme alone is irradiated or if enzyme plus **2** remains in the dark. These data indicate that the enzyme treated with the photoaffinity label in the dark exhibits full activity because the dilution procedure completely dissociated noncovalently bound **2**. RT-1 activity, however, decreases in a time-dependent irreversible manner as enzyme plus **2** is irradiated. The nonlinear curve of the photolabeling suggests that the fraction of decomposed free **2** during the experiment was not negligible. Therefore, in order to achieve a pseudo-first-order rate, the ratio of **2**/RT-1 was increased and initial rates were measured.

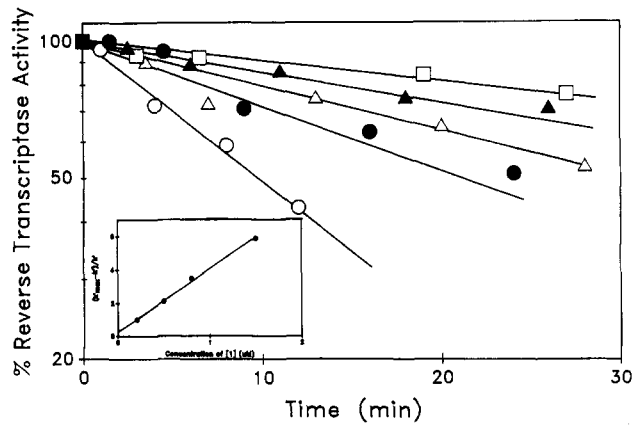

FIGURE 2: Protection of RT-1 from photoinactivation. The irreversible photoinactivation of RT-1 (0.4 μM) by **2** (0.9 μM) in the presence of various concentrations of **1** [(○) 0, (●) 0.2, (△) 0.5, (▲) 0.8, and (□) 1.5 μM] was followed as described in Figure 1B. Kinetic parameters $(k'_{max} - k')/k'$ obtained were plotted against the concentration of **1**, as presented in the inset figure, according to eq 1.

Protection of RT-1 from Photoinactivation. In order to examine whether the photoaffinity label was bound to the same site as **1**, RT-1 was irradiated in the presence of a fixed concentration of **2** and varying concentrations of **1**. As shown in Figure 2, the photoaffinity labeling was retarded by the presence of **1**. As the concentration of **1** was varied from 0 to 1.5 μM, the enzyme was increasingly protected from irreversible inactivation. Thus, **1** acts as a competitive inhibitor of the photoinactivation reaction. From the slopes obtained from Figure 2, the apparent rate constant k' at corresponding protector **1** concentrations was calculated. Using eq 1 (Wu

$$\frac{1}{k'} = \frac{1}{k'_{max}}\left[1 + \frac{K_2}{[2]}\left(1 + \frac{[1]}{K_1}\right)\right] \qquad (1)$$

et al., 1989) and plotting the calculated $(k'_{max} - k')/k'$ values versus the concentration of **1** give results shown in the inset of Figure 2, where k'_{max} represents the rate constant of photoinactivation at a given concentration of **2** ≫ RT-1 and **1** = 0. The linearity of the plot suggests that **1** indeed competes with the photoaffinity label for the same binding site on RT-1. The dissociation constants of **2** (K_2) and **1** (K_1) were calculated according to eq 1 (K_2 = 250 nM; K_1 = 79 nM). These kinetic parameters were found to be consistent with IC_{50} values for **2** and **1** for the inhibition of RT-1 in the dark (160 and 90 nM, respectively) (Figure 1A).

When similar photolabeling studies were carried out with other diazepinone analogues (**5**–**7**) as competitors, the extent of protection correlated closely with the IC_{50} values of the compounds (Figure 3). Interestingly, the TIBO compound **4** was also found to competitively protect RT-1 from photoinactivation by **2**. The dissociation constant for binding was calculated to be 195 ± 20 nM from the data analysis method described in Figure 2 (data not shown). When enzyme substrates, i.e., tRNA, poly(rC)·oligo(dG), or dGTP, were tested

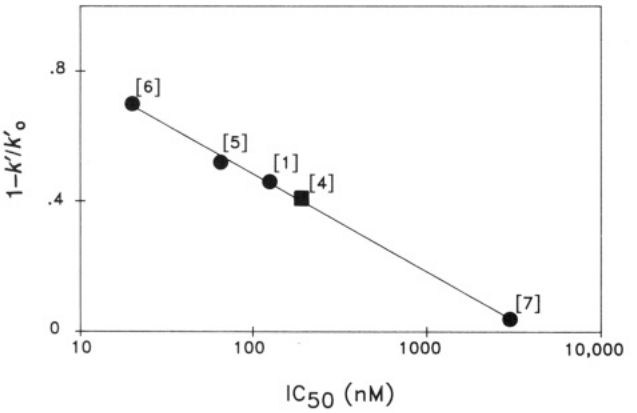

FIGURE 3: Protection of RT-1 from **2** by different dipyridodiazepinone analogues and TIBO (**4**). RT-1 (0.4 μM) was photolabeled with **2** (0.9 μM) in the presence of the indicated dipyridodiazepinone analogues (●) or TIBO (**4**) (■). The degree of protection is expressed as $1 - k'/k'_0$ and plotted against IC_{50} values of each compound; k' and k'_0 represent the rate constants of photolabeling in the presence or absence of protector, respectively.

Table I: Effects of Enzyme Substrates and TIBO (**4**) on the Photolabeling of RT-1 by **2**[a]

reagent	concn	$1 - k'/k'_0$
1	0.9 μM	0.64
4	0.9 μM	0.43
yeast tRNA	0.2 mg/mL	−0.15
poly(rC)/oligo(dG)	10 μg/mL	−0.31
dGTP	10 μM	−0.28

[a] Experimental procedures are the same as described in Figure 3.

as competitors, no protection of RT-1 was observed. In fact, a slight enhancement in the rate of photoinactivation was observed (Table I).

Stoichiometry and Specificity of Photoaffinity Labeling. Tritiated photoaffinity label **3** was synthesized in order to correlate the degree of RT-1 inhibition (r) with the number (n) of covalent labels attached to the enzyme. As shown by Figure 4A, the correlation is clearly biphasic: first, the labeling of RT-1 (1.23 μM) by **3** (3.5 μM) proceeded with $dr/dn \approx -1$ until $n \approx 1$; then, after the additional introduction of **3** in high excess (28.8 μM), the labeling continued with $dr/dn \approx 0$. The slope $dr/dn \approx -1$ indicates that the first phase of labeling is highly specific; i.e., every mole of label that covalently attached to RT-1 inactivated 1 mol of enzyme.

RT-1 is a heterodimer composed of 51- and 66-kDa subunits (p51 and p66). SDS–polyacrylamide gel electrophoresis analysis indicated that the RT-1 heterodimer is only labeled on the p66 subunit by **3** during the first phase of photoaffinity labeling (Figure 4B). The p66-labeled heterodimer can be further labeled by adding a large excess of **3** at the end of the first phase when $n \approx 1$ (25 min). As illustrated by Figure 4B, this additional incorporation of **3** was covalently associated with both p51 and p66 subunits and is apparently nonspecific. Quantitative data supporting this conclusion were obtained by photoaffinity labeling RT-1 in the presence of **3** for various times, subjecting the samples to SDS–PAGE, cutting out the stained protein bands corresponding to each subunit, and determining the associated photoaffinity label by liquid scintillation counting (Figure 4B). The preferential association of **3** with p66 over p51 is evident at short illumination times and at low concentration of the photoaffinity label, whereas p51 became labeled only at longer times and higher concentration. When a mixture containing approximately 1% RT-1 and 99% human leukocyte cytosolic proteins was exposed to 3.2 μM **3** under UV light, only the p66 subunit of RT-1 was

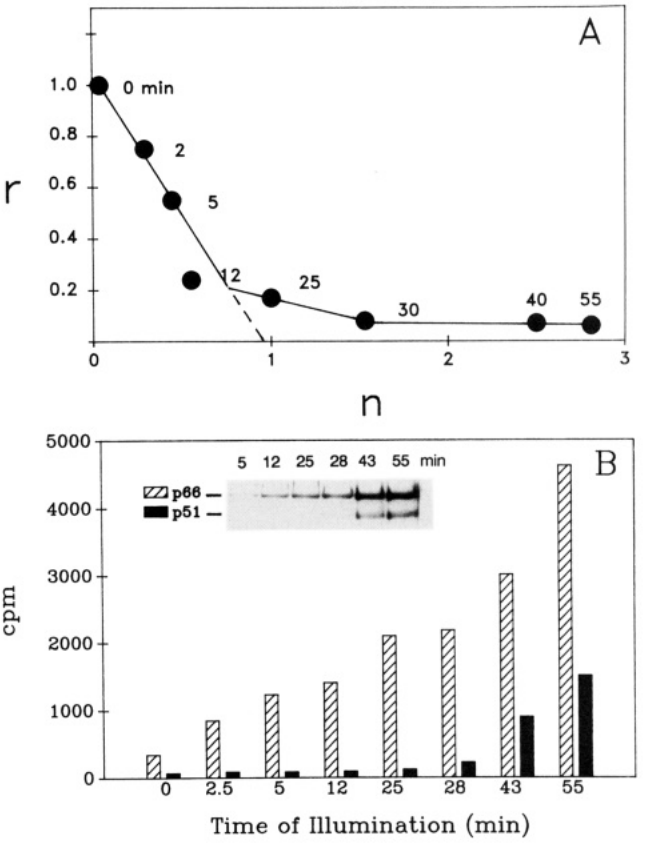

FIGURE 4: Stoichiometry and localization of photoaffinity labeling on RT-1. (A) Correlation between the inhibition of RT-1 and bound label. A 1.2 μM RT-1 solution in 50 mM Tris-HCl buffer, pH 7.8, was photoirradiated at an intensity of 15 $\mu W/cm^2$ in the presence of 3.5 μM **3**. After 0, 2, 5, 12, and 25 min of illumination, aliquots were removed from the irradiated solution and centrifugally gel-filtered through Sephadex G-50. The filtrate was assayed for radioactivity, enzyme activity, and protein concentration. At $t = 0$, n was found to be 0.06, suggesting that this procedure is sufficient for separating noncovalently bound **3** from RT-1. The second addition of **3** in large excess (28.8 μM) was introduced to the photoreaction mixture at 25 min. r = ratio of the specific activity of labeled RT-1 to that of the unlabeled enzyme; n = moles of the covalently attached **3** per mole of RT-1. The specific radioactivity of **3** was 2.02 Ci/mmol, and the radioactivity of the filtrate was usually found to be $(1–10) \times 10^3$ cpm per 3-μL aliquot, depending on the protein concentration and the time of the UV illumination. (B) SDS–PAGE analysis of labeled RT-1. The photoirradiated reaction mixture prepared as in (A) was collected at the times indicated, and 1.2 μg of the photolabeled RT-1 was analyzed by SDS–PAGE. The gel was stained, the bands corresponding to p66 and p51 subunits were cut out, and radioactivity was measured. An autoradiograph of the gel after a 4-day exposure (see Materials and Methods) is presented in the inset.

photolabeled (Figure 5). This provides compelling evidence that RT-1 is the only significant target for the photoaffinity label in a whole cell lysate. When BSA and RT-2 were treated with 3.2 μM **3** under the same conditions, the BSA and both p54 and p68 subunits of RT-2 were labeled, but far less extensively than the labeling achieved on RT-1.

Discussion

In the present work, we have demonstrated that BI-RG-587, a dipyridodiazepinone (**1**), and the structurally related photoaffinity analogue **2** in the dark inhibit RT-1 polymerase activity in a reversible fashion. This inhibition is highly specific since RT-2, a highly homologous enzyme, is not affected by **1** and **2**. Further support for the inhibitory specificity has been demonstrated by Merluzzi et al. (1990), where compound **1** was found to be inactive against calf thymus and human DNA polymerases.

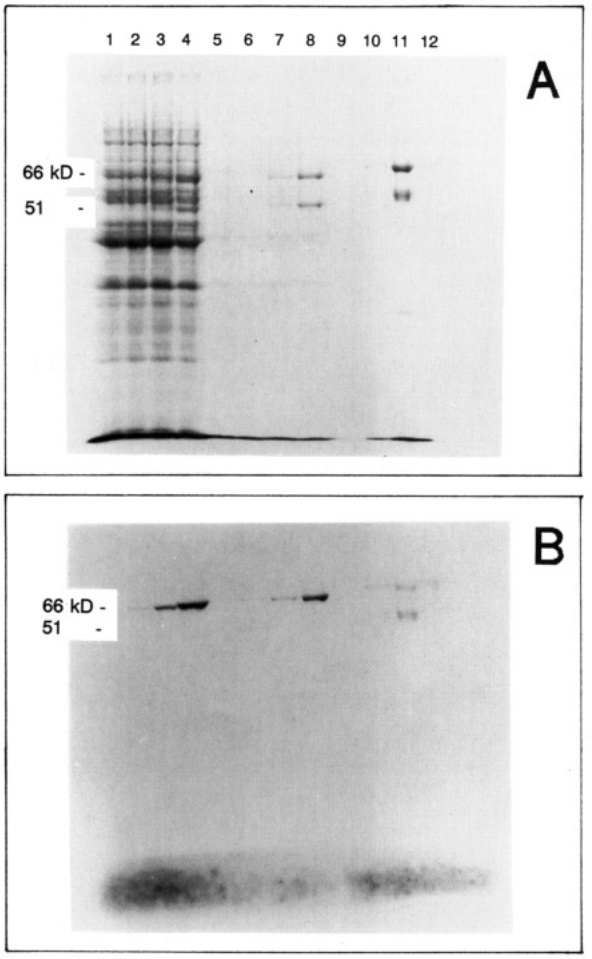

FIGURE 5: Specificity of RT-1 photolabeling. Purified RT-1 was mixed with cytosolic proteins from human peripheral blood leukocytes (PBL) and radiolabeled with the photoaffinity probe **3** at approximately 3.5 μM with 30 min of UV irradiation. RT-2 and BSA were also subjected to photoaffinity labeling with **3**. SDS–PAGE using 10% gels was performed on the samples. Panels A and B show respectively the gel stained with Coomassie blue and the corresponding autoradiograph. Lanes 1, 2, 3, and 4 contained 100 μg of PBL protein with 0, 0.2, 1, and 5 μg of RT-1, respectively. Lanes 5, 6, 7, and 8 contained 10 μg of PBL protein with 0, 0.2, 1, and 5 μg of RT-1, respectively. Lanes 9, 10, and 11 contained 0.2, 1, and 5 μg of RT-2, respectively. Lane 12 contained 4 μg of BSA.

RT-1 was irreversibly inhibited by the azido photoaffinity label **2** following UV irradiation, whereas enzyme irradiated without **2** under identical conditions was unaffected. Azido photoaffinity probes decompose to highly reactive nitrenes under UV light that are capable of inserting into proximal covalent bonds of the protein backbone and amino acid side chains. Compound **1** was found to protect RT-1 competitively from photoinactivation by **2**. Several active diazepinone analogues protected RT-1 from irreversible inactivation, and the extent of protection was directly correlated with the IC_{50} value. Pauwels et al. (1990) have reported a series of non-nucleoside compounds that inhibit HIV-1 with high potency and selectivity, resembling the profile of **1**. This prompted us to investigate whether a representative TIBO derivative (**4**) might share a common binding site with **1** on RT-1. In protection experiments, **4** competitively protected RT-1 from photoinactivation by **2**. This observation suggests the existence of a modulatory site (RT_1MS) that, when occupied by an appropriate compound, inhibits the polymerase activity of the enzyme. RT_1MS is apparently distinct from the substrate binding site since tRNA, template-primer, and dGTP do not protect the enzyme from photoinactivation. This contention is further supported by a kinetic analysis in which **1** was shown to be a noncompetitive RT-1 inhibitor (Merluzzi et al., 1990).

A radiolabeled photoaffinity probe (**3**) was synthesized and used to correlate the degree of enzyme inhibition with the number of covalent labels attached to RT-1. It was found that 1 mol of **3** was sufficient to completely inhibit 1 mol of enzyme. Analysis of the photoaffinity-labeled enzyme by SDS–PAGE showed that the label was preferentially associated with the p66 subunit. The p51 subunit of RT-1 and both the p54 and p68 subunits of RT-2 are apparently only labeled in a non-specific fashion at high concentrations of **3**. The photoaffinity labeling of RT-1 is highly specific, since even in the presence of a 100-fold excess of cytosolic proteins from human peripheral blood leukocytes only the p66 subunit was labeled.

ACKNOWLEDGMENTS

We thank Dr. S. J. Benkovic for helpful discussions. We also thank Sheri Rogers for technical assistance and Kathy Stewart for preparing the manuscript.

REFERENCES

D'Aquila, R. T., & Summers, W. (1989) *J. Acquired Immune Defic. Syndr. 2*, 579–587.
DeClercq, E. (1989) *Antiviral Res. 12*, 1–20.
DeClercq, E. (1990) *Trends Pharmacol. Sci. 11*, 198–205.
Fauci, A. S. (1988) *Science 239*, 617–622.
Guyader, M., Emerman, M., Sonigo, P., Clavel, F., Montagnier, L., & Alizon, M. (1987) *Nature 326*, 662–669.
Hao, Z., Cooney, D. A., Hartman, N. R., Perno, C.-F., Fridland, A., DeVico, A. L., Sarngadharan, M. G., Broder, S., & Johns, D. G. (1988) *Mol. Pharmacol. 34*, 431–435.
Hargrave, K. D., Proudfoot, J. R., Grozinger, K. G., Cullen, E., Kapadia, S. R., Patel, U. R., Fuchs, V. U., Mauldin, S. C., Vitrous, J., Pal, K., Behnke, M. L., Skiles, J. W., Klunder, J. M., McNeil, D. W., Rose, J. M., Chow, G., Skoog, M. T., Wu, J. C., Schmidt, G., Engel, W. W., Eberlein, W. G., Saboe, T. D., Campbell, S. J., & Adams, J. (1991) *J. Med. Chem.* (in press).
Laemmli, U. K. (1970) *Nature 227*, 680–685.
Larder, B. A., & Kemp, S. D. (1989) *Science 246*, 1155–1158.
Merluzzi, V. J., Hargrave, K. D., Grozinger, K., Labadia, M., Eckner, K., Hattox, S., Adams, J., Rosenthal, A. S., Faanes, R., Skoog, M., Wu, J. C., Shih, C.-K., Eckner, R., Koup, R. A., & Sullivan, J. L. (1990) *Science 250*, 1411–1413.
Mizrahi, V., Lazarus, G. M., Miles, L. M., Meyers, C. A., & Debeouck, C. (1989) *Arch. Biochem. Biophys. 273*, 347–358.
Pauwels, R., Andries, K., Desmyter, J., Schols, D., Kukla, M. J., Breslin, H. J., Raeymaeckers, A., VanGelder, J., Woesteinborghs, R., Heykants, J., Schellekens, K., Janssen, M. A., DeClercq, E., & Janssen, P. A. (1990) *Nature 343*, 470–474.
Richman, D. D., Fischl, M. A., Grieco, M. H., Gottlieb, M. S., Volberding, P. A., Laskin, O. L., Leedom, J. M., Groopman, J. E., Mildvan, D., Hirsch, M. S., Jackson, G. G., Durack, D. T., & Lehrman-Nusinoff, S. (1987) *N. Engl. J. Med. 317*, 192–197.
Starnes, M. C., & Cheng, Y.-C. (1987) *J. Biol. Chem. 262*, 988–991.
Wu, J. C., Chuan, H., & Wang, J. H. (1989) *J. Biol. Chem. 264*, 7989–7993.